Received: 13 December 2019 | Revised: 21 February 2020 | Accepted: 24 February 2020 | Published online: 19 May 2020

DOI: 10.1002/dad2.12032

Alzheimer's & Dementia
Diagnosis, Assessment & Disease Monitoring

NEUROIMAGING

Impaired perfusion and capillary dysfunction in prodromal Alzheimer's disease

Rune B. Nielsen[1] | **Peter Parbo**[2] | **Rola Ismail**[2] | **Rikke Dalby**[1,7] | **Anna Tietze**[3] | **Hans Brændgaard**[4] | **Hanne Gottrup**[4] | **David J. Brooks**[2,5,6] | **Leif Østergaard**[1,2] | **Simon F. Eskildsen**[1]

[1]Center of Functionally Integrative Neuroscience, Aarhus University, Aarhus, Denmark

[2]Department of Nuclear Medicine and PET Centre, Aarhus University Hospital, Aarhus, Denmark

[3]Charité, Universitätsmedizin, Institute of Neuroradiology,, Berlin, Germany

[4]Dementia Clinic, Department of Neurology, Aarhus University Hospital, Aarhus, Denmark

[5]Division of Neuroscience, Department of Medicine, Imperial College London, London, UK

[6]Division of Neuroscience, Newcastle University, Newcastle upon Tyne, UK

[7]Department of Neuroradiology, Aarhus University Hospital, Aarhus, Denmark

Correspondence
Rune B. Nielsen, Center of Functionally Integrative Neuroscience, Department of Clinical Medicine, Aarhus University, Nørrebrogade 44, Building 1A, 8000 Aarhus C, Denmark.
Email: runebaeksager@me.com

Funding information
The Danish Council for Independent Research, Grant/Award Number: DFF-4004-00305; Danish Strategic Research Council, Grant/Award Number: 3056-00001

Abstract

Introduction: Cardiovascular disease increases the risk of developing Alzheimer's disease (AD), and growing evidence suggests an involvement of cerebrovascular pathology in AD. Capillary dysfunction, a condition in which capillary flow disturbances rather than arterial blood supply limit brain oxygen extraction, could represent an overlooked vascular contributor to neurodegeneration. We examined whether cortical capillary transit-time heterogeneity (CTH), an index of capillary dysfunction, is elevated in amyloid-positive patients with mild cognitive impairment (prodromal AD [pAD]).

Methods: We performed structural and perfusion weighted MRI in 22 pAD patients and 21 healthy controls.

Results: We found hypoperfusion, reduced blood volume, and elevated CTH in the parietal and frontal cortices of pAD-patients compared to controls, while only the precuneus showed focal cortical atrophy.

Discussion: We propose that microvascular flow disturbances antedate cortical atrophy and may limit local tissue oxygenation in pAD. We speculate that capillary dysfunction contributes to the development of neurodegeneration in AD.

KEYWORDS

Alzheimer's, amyloid, blood flow, capillary transit-time heterogeneity, dementia, hypoxia, mild cognitive impairment, magnetic resonance imaging, neurovascular, positron emission tomography, prodromal

1 | INTRODUCTION

Alzheimer's disease (AD) is the most common form of dementia, characterized by progressive cognitive decline and brain atrophy. The defining pathological features of AD include extracellular accumulation of β-amyloid-42 (Aβ) protein plaques and neurofibrillary tau tangles,[1] but changes in neurovascular morphology and function are also associated and could contribute to the development of the disease.[2-4] While reduced cerebral blood flow (CBF) can be observed in mild cognitive impairment (MCI) in the years before a clinical diagnosis of AD is made,[5,6] macroscopically, the nutritional blood supply appears to be coupled to metabolic needs and does not fall to ischemic levels. Microscopically, however, capillary flow heterogeneity may lead to local ischemia[7] and currently the exact role of cerebrovascular pathology in the development of AD remains unclear.

Cerebrovascular disease pathology is normally considered in the context of flow-limiting arterial stenosis and occlusions causing hypoperfusion to the extent that brain oxygen availability becomes limited and energy metabolism threatened. While CBF determines macroscopic tissue oxygen supply, the local extraction of oxygen is also contingent on blood being homogenously distributed across capillaries on a microscopic scale.[7,8] Accordingly, disturbed capillary morphology and function[9] may limit blood flow through some capillaries, while allowing a disproportionate fraction of the blood supply to be "shunted" through others causing flow heterogeneity—so-called capillary dysfunction. According to biophysical models, the resulting impairment of tissue uptake may be severe enough to cause local tissue ischemia at a microscopic level,[10] even in conditions in which CBF measures above ischemic levels. Notably, as capillary function deteriorates, the models also predict that tissue oxygenation can be maintained by raising rather than lowering the blood's capillary transit time, thereby allowing greater blood-tissue diffusion exchange to occur. Observations of decreasing temporo-parietal CBF in prodromal AD (pAD) may thus reflect an attempt to maintain oxygen extraction during capillary dysfunction.[11]

To detect this capillary dysfunction and estimate its effects on local oxygen availability, one can extend classical neuroimaging-based measurements of tissue perfusion, such as CBF and mean transit time (MTT),[12] with information about the capillary transit-time heterogeneity (CTH)—the standard deviation of blood's transit times as it flows through the microvasculature.[13] With estimates of capillary MTT and CTH, the balance between local oxygen availability and metabolic demands can be computed as the tissue oxygen tension (P_tO_2) that results from cerebral oxygen utilization.[7,10,14]

We recently reported that CTH is elevated relative to MTT in patients with AD compared to healthy, age-matched controls with no history of vascular risk factors.[15] Notably, elevated CTH and reduced P_tO_2 were associated with more severe cognitive symptoms in patients with AD, and regional changes in indices of capillary dysfunction over a 6-month period were found to parallel deteriorating cognitive scores.[16] The current study examines whether subjects with pAD—amyloid positive MCI—also show evidence of capillary dysfunction (elevated CTH) and hypoperfusion (diminished CBF, prolonged MTT), compared with healthy, age-matched control subjects.

HIGHLIGHTS

- Elevated capillary transit time heterogeneity (CTH) limits local oxygen extraction
- Patients with mild cognitive impairment had elevated cortical CTH and amyloid load
- Hypoperfusion and reduced blood volume overlapped regions of elevated CTH
- Elevated CTH and hypoperfusion jointly reduced cortical tissue oxygen utilization
- Elevated CTH may be an overlooked therapeutic target in early Alzheimer's disease

RESEARCH IN CONTEXT

1. Systematic review: The authors used traditional online search engines to identify published studies on Alzheimer's disease (AD) etiology and capillary dysfunction—a condition wherein capillary blood flow disturbances limit oxygen extraction, rather than blood supply. The authors noticed that the condition could be a hitherto overlooked vascular contributor to the development of AD.
2. Interpretation: Their findings suggest that cortical microvascular blood flow disturbances and concurrent hypoperfusion combine to reduce tissue oxygenation, putatively preceding cortical atrophy, in amyloid-β positive mild cognitive impairment patients.
3. Future directions: Replication of the findings in longitudinal cohorts of healthy subjects at risk of developing AD is required to determine the role of capillary dysfunction at presymptomatic disease stages. Because amyloid-β oligomers may cause capillary constriction via pericytes, studies should interrogate the cause of capillary dysfunction with a particular focus on its association with cerebral amyloid-β accumulation and AD risk factors.

2 | MATERIALS AND METHODS

This study is part of an ongoing longitudinal study designed to evaluate relationships among cerebral neurodegeneration, perfusion, inflammation, and protein deposition in subjects with MCI and in healthy controls. Subjects were recruited between November 2013 and March 2017. The Regional Ethics Committee for Biomedical Research in the Central Denmark Region approved the study [1-10-72-116-13] and participants provided informed written consent. The study was carried out subsequent to our previous studies on capillary dysfunction in separate and independent patient cohorts with dementia.[15,16]

2.1 | Subjects

MCI subjects were recruited through newspaper advertisements and from national dementia and memory clinics. Inclusion criteria were a corroborated history by friends and carers of declining memory

function for at least 6 months; age of 50 to 85 years; fulfillment of the Petersen criteria[17] for MCI (no strict memory score cut-off was required); at least 7 years of education or a good working history; an accompanying informant able to describe the subject's memory condition and assist in the Clinical Dementia Rating (CDR); Mini-Mental State Examination (MMSE) score of 24 to 30; and a magnetic resonance imaging (MRI) examination that excluded MCI arising from structural lesions. Exclusion criteria were depression (Geriatric Depression Scale [GDS-15] score above 6); stroke or systemic diseases; modified Hachinski Ischemic Scale score above 4; contraindications to gadolinium contrast agent and MRI; significant neurological or psychiatric disease; history of alcohol and/or recreational drug abuse within 2 years; significant reductions in serum B12, red cell folate, thyroid or renal function; use of sedative medication and use of medication within the past 3 months with either anticholinergic effects or a negative influence on cognition.

Healthy age-matched control subjects were recruited through newspaper advertisements, following enrolment criteria identical to those for MCI but without complaints of memory decline and no indications of significant cognitive impairments on their neuropsychological screening.

2.2 | Neuropsychological assessment

All subjects underwent standardized neuropsychological assessments recommended for monitoring cognitive functioning in MCI and dementia.[18] Here, we present summary scores for MMSE, CDR Sum-Of-Boxes, and for the GDS-15 depression-screening tool. Trained research assistants conducted the neuropsychological assessments under the supervision of an experienced neuropsychologist.

2.3 | MRI acquisitions

MRI was performed on a 3T Skyra system (Siemens Healthcare, Erlangen, Germany) using a 32-channel head coil.

Structural 3D T_1-weighted (T_1w) MP2RAGE (magnetization-prepared two rapid gradient echo acquisitions)[19] images were acquired with 1.0 mm isotropic voxels.

T_2-weighted fluid attenuated inversion recovery (T_2w-FLAIR) images with $0.7 \times 0.7 \times 3.0$ mm^3 voxels were acquired to identify white matter hyperintensities (WMH) and, in conjunction with the MP2RAGE, to exclude structural abnormalities.

Dynamic susceptibility contrast (DSC) MRI with gradient echo (GE) and spin echo (SE) acquisition was applied to measure total vascular and microvascular blood volume and hemodynamics. GE DSC-MRI was acquired by echo-planar imaging (EPI; 300 volumes with 3 mm isotropic voxels in 29 slices without gap). Then, SE DSC-MRI was conducted by EPI (300 volumes with 3 mm isotropic voxels in 19 slices with 1 mm slice-gap); 0.1 and 0.2 mmol/kg gadobutrol (Gadovist, Bayer®, HealthCare Pharmaceuticals, Berlin) was injected during the GE and SE acquisitions, respectively. The supporting information provides additional details regarding MRI acquisitions.

2.4 | Positron emission tomography amyloid imaging and amyloid status

Brain Aβ load were assessed with positron emission tomography (PET) using a High-Resolution Research Tomograph (ECAT HRRT; CTI/Siemens) and ^{11}C-Pittsburgh Compound B (PiB). The supporting information provides additional details regarding PET acquisitions and preprocessing.

Utilizing MINC-tools,[20] PET images were co-registered to the T_1w MRI scan and non-linearly transformed into MNI-space (Montreal Neurological Institute) to achieve spatial normalization. PET images were then summed from 60 to 90 minutes post injection and the resulting images divided by the mean cerebellar gray matter signal,[21] to generate PiB standard uptake value ratio (SUVr) maps. Then, each patient's composite cortical PiB-SUVr level was calculated as the weighted average of PiB-SUVr levels across bilateral inferior/lateral parietal, inferior frontal, middle/inferior temporal, posterior cingulate, and parahippocampal cortices as defined by an atlas.[21] Finally, patients were defined as either amyloid positive (Aβ+) or amyloid negative (Aβ-) based on their composite cortical PiB-SUVr lying above or below 1.5. A threshold of 1.5 was selected as this naturally divided the bimodal distribution of composite cortical SUVrs into high and low subgroups.[18]

2.5 | Structural image processing

Using the framework described by Aubert-Broche et al.,[22] T_1w images were denoised, bias field corrected, registered to MNI space, and skull-stripped. Brain tissue was then segmented into gray matter, white matter, and cerebrospinal fluid.

To detect cerebral atrophy in MCI subjects, their hippocampal volume and cortical thickness were compared to the means of age-matched healthy controls. Total hippocampal volume was measured from automatically defined[23] bilateral hippocampus segmentations (Figure 1A). Subject-specific total intracranial volume was used for normalization. Cortical thickness was determined as the perpendicular distance between the inner and outer cortical boundary (Figure 1B), automatically delineated[24] on the T_1w images.

WMH load was measured as the combined volume of periventricular and subcortical T_2w-FLAIR WMHs (Figure 1C), relative to the total intracranial volume. WMHs were automatically segmented using a histogram based method[25] followed by a region growing algorithm. A mask of normal appearing white matter (NAWM) was then defined by removing WHMs from the white matter classification.

2.6 | Perfusion analysis

DSC-MRI perfusion scans were slice-time and motion-corrected and co-registered to the T_1w image using SPM (The Wellcome Trust

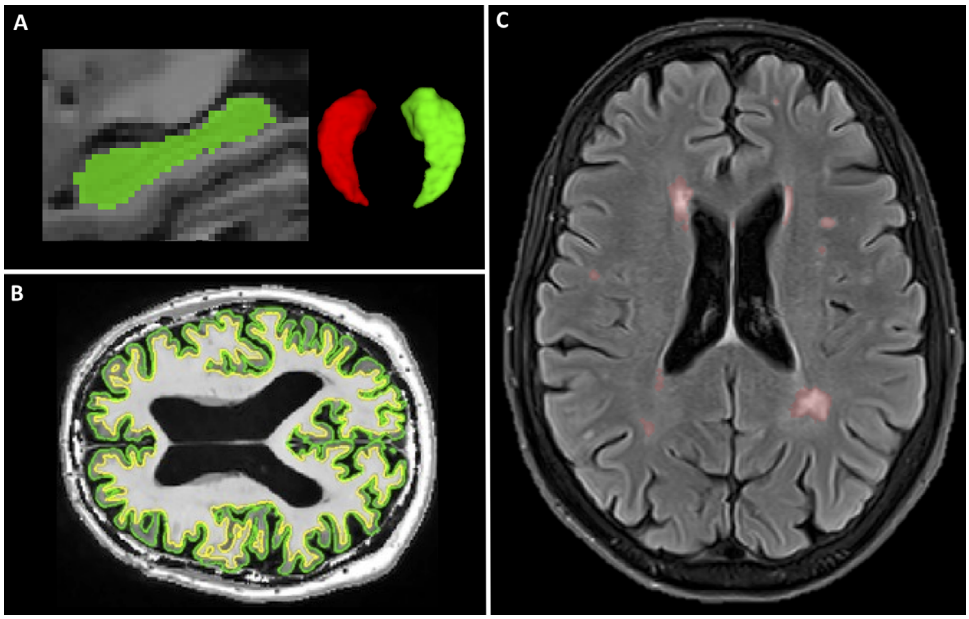

FIGURE 1 Cortical surface delineation and segmentation of hippocampi and white matter hyperintensities. Subject examples of A: the segmentation used for hippocampal volume measurements (red = left hippocampus, green = right hippocampus), B: the delineated inner and outer surfaces used to measure cortical thickness, and C: segmentation used for measuring white matter hyperintensity volume overlaid the T_2-weighted fluid attenuated inversion recovery (T_2w-FLAIR) image

Centre for Neuroimaging, University College London). Maps of CBF, cerebral blood volume (CBV), MTT, and CTH, were calculated by parametric deconvolution,[13] using NAWM as reference for the normalizations of relative metrics (CBF and CBV). Guided by an automated selection algorithm,[27] arterial input functions, which account for the arterial delivery of contrast medium, were manually selected within a region containing the middle cerebral arteries and its branches.

SE DSC-MRI is primarily sensitive to contrast medium in capillary-sized vessels,[28,29] whereas GE DSC-MRI is equally sensitive to contrast medium across all vessel sizes.[28] Therefore, SE-based CBV is often used as a surrogate for capillary density, whereas GE-based CBV characterizes the entire blood volume. The relative transit time heterogeneity (RTH equal to CTH/MTT), tends to remain constant across brain tissue types in healthy subjects.[15,30] We generated maps of RTH in our subjects to examine whether RTH is altered in MCI. While GE-based MTT, CTH, and RTH measurements are expected to reflect perfusion and perfusion heterogeneity across all levels of the vascular tree represented within an image voxel, SE-based measurements reflect mainly capillary hemodynamics, which, in turn, determine oxygen extraction efficiency. Notice that all the perfusion indices pertain to single voxels. Hence, CTH and MTT characterizes blood transit times across single voxels, rather than from say arteriole to exiting vein.

2.7 | Estimating brain oxygenation

To index local, voxelwise oxygen availability, we applied a biophysical model[7] that estimates the tissue oxygen tension (P_tO_2) that would result if local hemodynamics, as determined by SE-based MTT and CTH values, were to support the normal resting oxygen utilization of brain tissue, 2.5 mL/100 mL/min.[31] Following,[13] we assumed a capillary blood volume of CBV = 4.0% and calibrated the biophysical model to yield an oxygen extraction fraction = 0.3 and P_tO_2 = 25 mmHg in NAWM.

2.8 | Extraction of cortical data

We transformed subject-specific cortical surface-segmentations (Figure 1B) into perfusion image native space. Each perfusion map was then interpolated and mapped to a surface approximating the middle cortical layer to minimize partial volume effects and noise caused by large vessels at the cortical surface.

To statistically interrogate inter-subject changes, perfusion surface values and cortical thickness values were mapped to a standard cortical surface in MNI space and blurred using a 20 mm full width half maximum geodesic Gaussian kernel to avoid blurring across gyri.[32]

2.9 | Statistical analysis

We used R v.4.3 (R Foundation for Statistical Computing, Vienna, Austria) for statistical interrogation of data for Aβ+ MCIs (pAD) and healthy controls. Between-group differences in demographics, cognitive test-scores, hippocampal volume, and WMH load were assessed according to variable-class and sample distribution behavior. An independent two-sample *t*-test was applied to compare means of normal distributed continuous variables, while skewed continuous or

TABLE 1 Demographics, neuropsychological test results, hippocampal volume, and WMH load

Participant characteristics	Aβ+ MCI (n = 22)	Healthy controls (n = 21)	*P* value
Age, years, mean ± SD [range]	72.9 ± 6.4 [62–85]	69.4 ± 5.9 [59–79]	.0687
Sex, females, n (%)	4 (18)	13 (62)	.0051
Education, years, mean ± SD	12.3 ± 2.9	13.5 ± 2.3	.1449
Subjects using NSAID, n (%)	7 (32)	4 (19)	.4876
Subjects using antihypertensive drugs, n (%)	10 (45)	5 (24)	.2027
MMSE score, mean ± SD [range]	26.5 ± 2.1 [21–30]	28.3 ±1.4 [26–30]	.0013
CDR sum of boxes, median [range]	1.5 [0.0–7.0]	0.0 [0.0–1.0]	<.0001
Geriatric Depression Scale, mean ± SD	2.0 ± 2.1	0.71 ± 1.62	.0301
Subjects with Fazekas score, 0/1/2/3, n	3/9/7/3	5/9/5/2	.2793
White matter hyperintensity volume, % ICV, median [Q_1–Q_3]	0.55 [0.3–1.3]	0.38 [0.2–0.7]	.1736
Hippocampal volume, mL, mean ± SD	5.16 ± 0.68	5.59 ± 0.53	.0291
PiB dose, MBq, mean ± SD	383 ± 68	413 ± 23[a]	.1440

NOTE: Four healthy controls did not complete the CDR because the required informant was not present. Based on an in-depth interview, their CDR sum of boxes score was set to zero. Each hippocampal volume was normalized to the subject total intracranial.
Abbreviations: Aβ+, PiB-positive; Aβ−, PiB-negative; CDR, Clinical Dementia Rating; ICV, total intracranial volume; MCI, mild cognitive impairment; MMSE, mini-Mental State Examination; NSAID, non-steroidal anti-inflammatory drug; PiB, Pittsburgh Compound B; Q_1, lower quartile; Q_2, upper quartile; SD, standard deviation; WMH, white matter hyperintensity.
[a]Twelve healthy controls had PiB-PET.

ordinal variables were interrogated using the Kruskal-Wallis test. Fischer exact test was applied to categorical variables and $P < .05$ was considered statistically significant. Cortical surface-based group comparisons of MRI-derived indices were conducted with a mass univariate vertex-wise approach, using linear regression to correct for possible age and sex differences. The resulting t-values for outcome variables were rendered on the cortical MNI surface template for $P < .05$ along with delineations of clusters surviving family-wise error (FWE) correction[33] at $\alpha = .001$. For each perfusion surface analysis, we defined a "most significant area" by detecting the highest t-value threshold that satisfied the cluster extend-threshold calculated with the FWE-correction. The resulting cluster masks were applied to extract mean parameter values within the "most significant area" for visualization purposes. The regional mean cluster values are shown using violin plots, including mean and 95% confidence intervals.

3 | RESULTS

Twenty-one healthy controls and thirty-five MCI cases were initially included in the study. Based on PiB-PET findings, 22 MCI subjects were classified as Aβ+ (pAD) and 13 MCI subjects as Aβ−. Two MCI cases, both classified as Aβ+, did not complete their SE perfusion MRI scan due to technical problems. Twelve age-matched controls had PiB-PET; two showing raised amyloid suggestive of preclinical AD while the other ten were Aβ−. Table 1 summarizes participant demographics for the resulting study population of 22 Aβ+ MCI patients and 21 healthy controls. The two groups had similar mean years of education and similar antihypertensive and non-steroidal anti-inflammatory drug use. Moreover, the groups were similar with regard to vascular brain lesion load; specifically, the Fazekas scale score and WMH volume. The Aβ+ MCI group was slightly older than controls though the difference was not significant, comprised significantly fewer females, performed significantly worse on the cognitive tests MMSE and CDR, and had smaller hippocampi compared to the control group. Additionally, the Aβ+ MCIs scored higher on the GDS test compared to controls.

3.1 | Cortical thickness

We found a trend toward focal cortical thinning in the Aβ+ MCI subjects compared with the controls (Figure 2). Specifically, a significant cluster of thinning located in the right precuneus close to the caudal part of the marginal gyrus survived FWE-correction.

3.2 | Perfusion and oxygenation group differences

Figures 3 and 4 show differences between the MCI group and the healthy control group in GE- and SE-based perfusion indices and SE-derived oxygenation, respectively. Frontal, parietal, and temporal cortical areas showed reduced CBF and CBV, and prolonged MTT in the Aβ+ MCI cases compared with controls as measured by GE DSC-MRI, which is equally sensitive to hemodynamics across all vessel sizes. MTT equals CBV/CBF[34] and is inversely related to regional perfusion pressure.[35] Overall, these findings are thus consistent with a relative vasoconstriction and concomitant hypoperfusion across these brain regions.

SE-based perfusion maps showed areas of reduced CBV in Aβ+ MCI cases compared with controls. Situated in close proximity of areas displaying GE-based CBV reductions after FWE-correction, these findings suggest that blood volume reductions include capillary capacity. Being weighted toward capillary-sized vessels, these reductions in CBV are

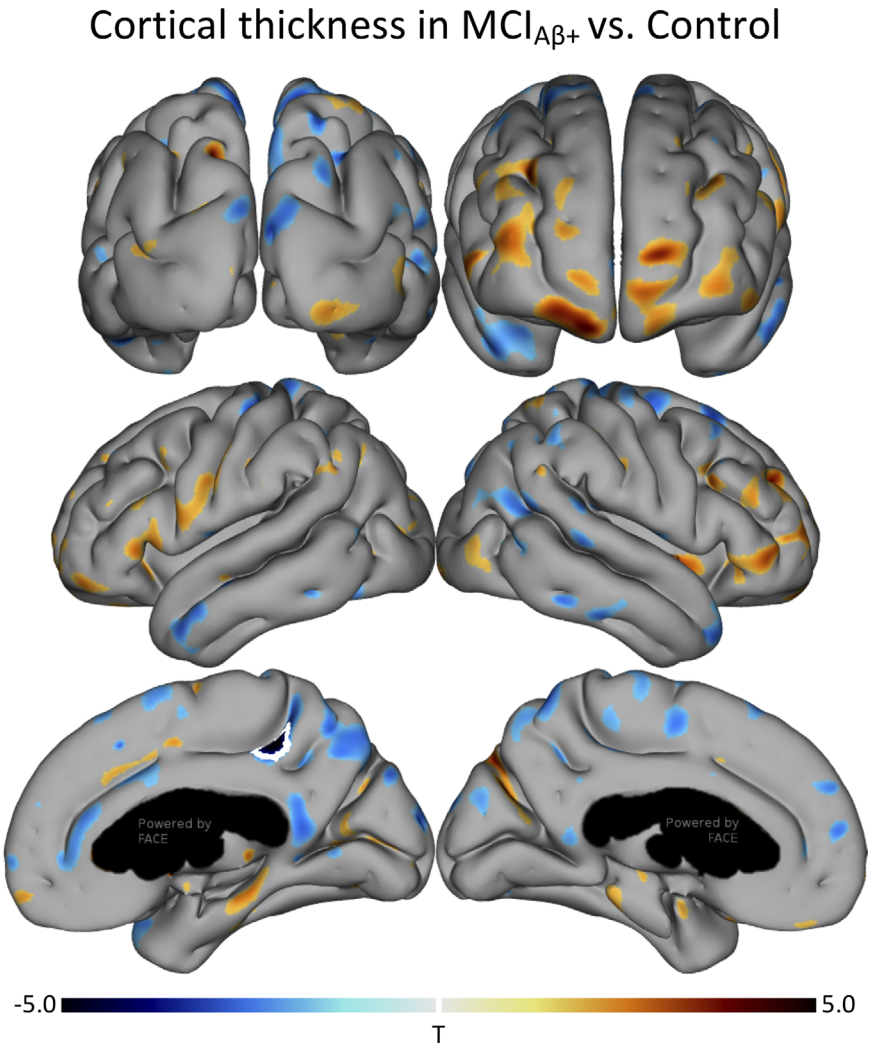

FIGURE 2 Cortical thickness in amyloid positive (Aβ+) subjects with mild cognitive impairment (MCI) compared with healthy controls. Statistical t-value maps are adjusted for age and sex using linear regression, and thresholded at $P < .05$. Negative t-values indicate reductions (blue nuances), while positive t-values indicate increases (red nuances) in the MCI group. The white outlines highlight clusters surviving family-wise error correction for multiple comparisons at $\alpha = .001$. Aβ+ was defined by an atlas based Pittsburgh Compound B standard uptake value ratio above 1.5, using mean cerebellar uptake for reference

consistent with capillary constrictions or even reduced capillary density. In Aβ+ MCI, SE-based CBF was reduced and MTT and CTH elevated across most of the cerebral cortex, leaving only the occipital lobe relatively unaffected.

There were no group differences in neither SE-based, nor GE-based RTH—the CTH:MTT ratio.

Oxygenation, as indexed by the P_tO_2 estimated from SE-based MTT and CTH measurements, was reduced in Aβ+ MCI across all major cortical lobes (Figure 4), with the most prominent reductions situated in the right lateral temporal cortex, and in the inferior prefrontal cortex. Temporal lobe P_tO_2 reductions coincided with identified increases in MTT and CTH, while the prefrontal reductions overlapped with regions of reduced CBF and CBV.

4 | DISCUSSION

The first key finding of this study is that pAD (MCI with raised amyloid load) is associated with widespread microvascular flow disturbances in addition to macroscopic cortical hypoperfusion. Utilizing DSC-MRI sensitized to capillary-sized vessels, we found areas of reduced microvascular blood volume in MCI compared to controls, suggesting that these microvascular flow disturbances are arising from capillary constrictions or capillary loss. The cause of these hemodynamic changes is unclear, but we note that AD risk factors such as cardiovascular ischemic disease and insulin resistance are associated with changes in capillary morphology and function,[11] and that Aβ oligomers constrict human capillaries by interfering with pericyte tone,[36] possibly heralding the pericyte loss observed in AD.[37] The MCI subjects in this study were selected on the basis of their high PiB uptake, but further studies need to examine the spatiotemporal relation between cortical amyloid retention and changes in microvascular CTH and CBV, respectively.

Our second key finding is that cortical microvascular flow disturbances in subjects with pAD are closely coupled to parallel increases in MTT and reduced CBF. Accordingly, the cortical distributions of the patients' SE-based MTT, CBF, and CBV changes were similar to that of their CTH changes, and their CTH:MTT ratios (RTH) remained unchanged from those of controls. The causal relation between elevated CTH on one hand, and the hypoperfusion in Aβ+ MCI subjects, on the other, is less clear. Biophysical models predict that when capillary flow disturbances, as indexed by CTH, reach a certain threshold, blood

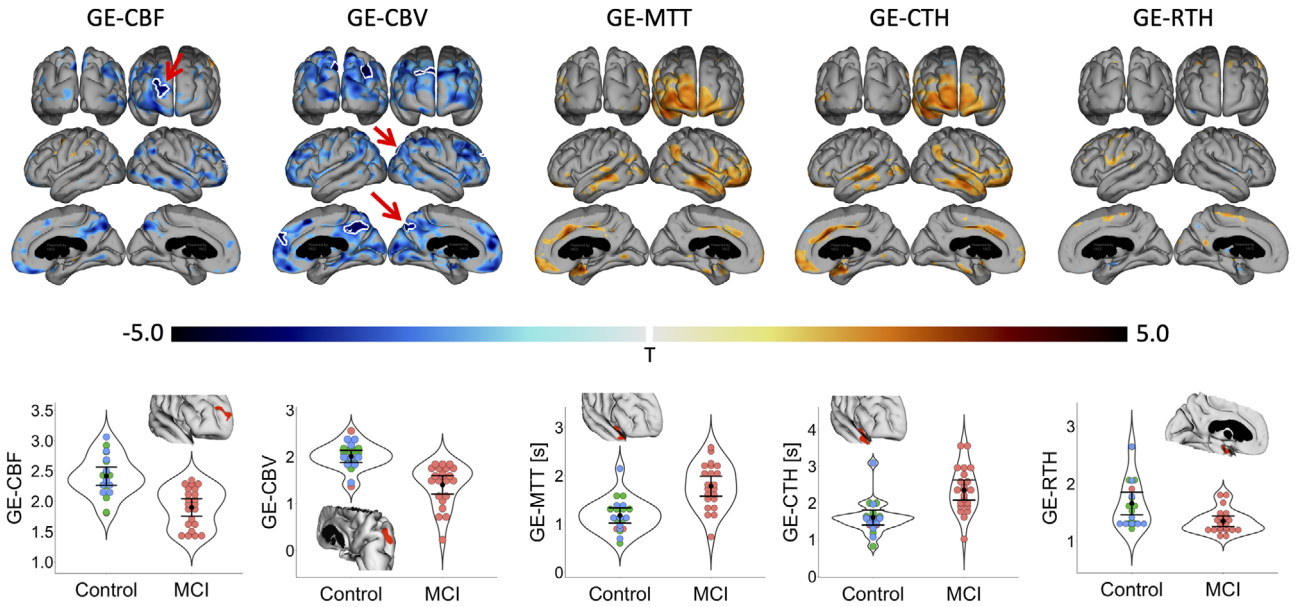

FIGURE 3 Elevated capillary transit time heterogeneity (CTH) accompanies reductions in cerebral blood flow (CBF) and cerebral blood volume (CBV) in amyloid positive (Aβ+) subjects with mild cognitive impairment (MCI) compared with controls. All measurements were acquired with gradient echo (GE) based perfusion weighted magnetic resonance imaging. Group differences in CBV extended across all four lobes with parietal and frontal clusters surviving family-wise error (FWE)-correction. For CBF, a single cluster in the right frontal lobe survived FWE-correction. Statistical t-value maps were adjusted for age and sex using linear regression and thresholded at $P < .05$. Negative t-values indicate reductions (blue nuances), while positive t-values indicate increases (red nuances) in the MCI group. The red arrows and the white outlines highlight clusters surviving family-wise error correction for multiple comparisons at $\alpha = .001$. Violin plots with group mean (black dot) and 95% confidence interval, show the region of interest means extracted from the most significant cluster or (in the case of no surviving clusters) the most significant region fulfilling the required minimum cluster extent-threshold. The regions of interest are highlighted in red on the smaller binary maps. Aβ+ was defined by an atlas based Pittsburgh Compound B standard uptake value ratio above 1.5, using mean cerebellar uptake for reference. MTT, mean transit time; RTH, relative transit-time heterogeneity (RTH = CTH:MTT)

supply must be attenuated to limit capillary "shunting" of oxygenated blood, to meet the metabolic demands of brain tissue.[7,14] The vasoconstriction observed in Aβ+ MCI subjects compared to controls may therefore act to maintain uninterrupted oxygen use, as capillary dysfunction grows more severe, at the expense of a falling P_tO_2.[11] Consistent with the notion that deteriorating capillary function limits tissue oxygenation in early AD, we have previously observed that CTH and RTH, the CTH:MTT ratio, correlate with symptom severity in AD.[15,16] Nevertheless, in the present study, Aβ+ MCI subjects' RTH was similar to that of controls, despite their higher CTH. We speculate that this is because the MTT increase that characterizes Aβ+ MCI subjects is associated with increased CTH, which tends to initially "pseudo-normalize" the CTH:MTT or RTH ratio before it subsequently rises with increasing capillary flow disturbances as pAD progresses to become dementia.

In microcirculations comprised by passive, compliant microvessels, MTT and CTH tend to change in proportion.[38] Vasoconstriction and prolonged MTT in Aβ+ MCI subjects might therefore be a primary event, rather than a compensatory adjustment to elevated CTH. Nonetheless, both hypoperfusion and elevated CTH in Aβ+ MCI subjects could result from cerebral amyloid angiopathy, a feature of AD pathology that affects the morphology and function of both arterioles and capillaries.[39] While exogeneous amyloid aggregates act as a powerful arterial and arteriolar vasoconstrictor,[40] endogenous amyloid does not stimulate arteriolar or venular constriction.[36] However, recent findings suggest that amyloid oligomers preferentially constrict capillaries via their action on pericytes,[36] reinforcing the need to further explore the consequences of capillary dysfunction in early AD. Studies of the spatiotemporal relation between cortical amyloid retention and changes in microvascular MTT and CTH, respectively, could further elucidate the effects of amyloid on capillary function.

Our biophysical models of tissue oxygenation take both blood supply (MTT and CBF) and its microscopic distribution (CTH) into account when calculating the reduction in P_tO_2 as tissue oxygen uptake becomes limited by microvascular shunting and constriction.[7] Based on their hemodynamic changes, the models predict that Aβ+ MCI subjects have widespread cortical reductions in P_tO_2 compared with controls. This finding is consistent with reported upregulation of serum 2,4-dihydroxybutanoic acid, a metabolite released as hypoxia activates alternative energy production pathways,[41] in MCI subjects who progressed to AD,[42] and with diminishing cerebral oxygen supply in pericyte-deficient mice.[43] It is of note that, comparing Aβ+ MCI to controls, we did not detect parallel cortical atrophy or extensive white matter lesions to account for their reduced memory function.

Our results are consistent with previous reports of elevated CTH and abolished functional hyperemia in aged wild type mice and aged mice with AD-like pathology, including Aβ plaques.[44] Similarly, oth-

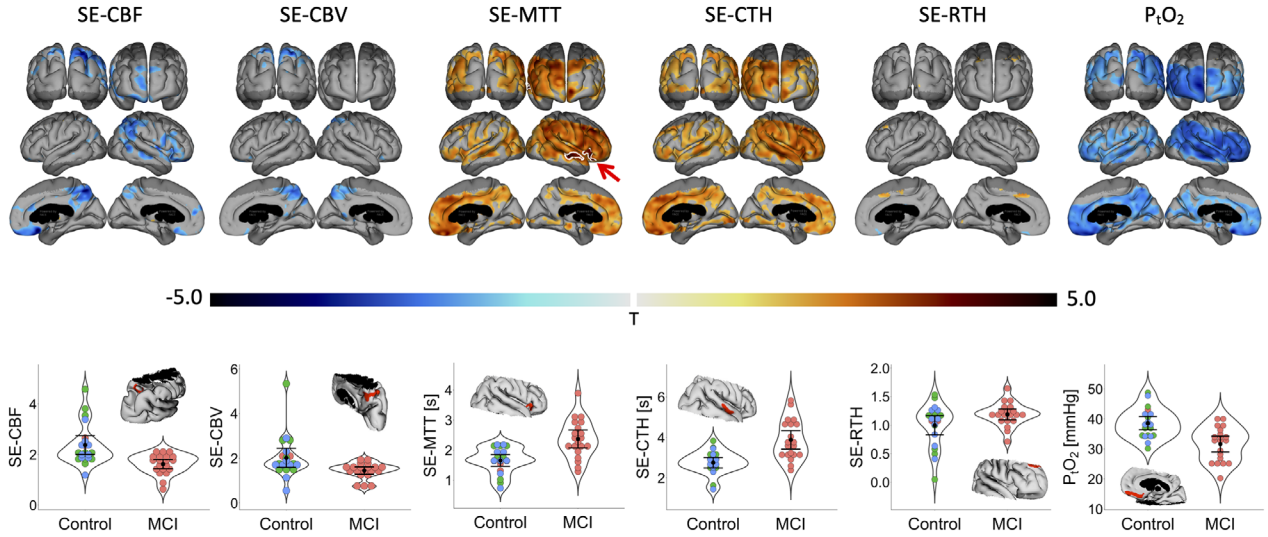

FIGURE 4 Reduced tissue oxygenation (P_tO_2) accompanies increased capillary transit time heterogeneity (CTH) and decreased microvascular perfusion in amyloid positive (Aβ+) subjects with mild cognitive impairment (MCI) compared with controls. All measurements were acquired with spin-echo (SE) based microvascular perfusion weighted magnetic resonance imaging. For Aβ+ MCIs, increases in mean transit time (MTT) in the frontal cortex and in the lateral temporal cortex survived family-wise error (FWE)-correction, while the largest increase in CTH and decrease in P_tO_2 occurred in the right superior temporal gyrus and medial inferior frontal cortex. Statistical t-value maps were adjusted for age and sex using linear regression and thresholded at $P < .05$. Negative t-values indicate reductions (blue nuances), while positive t-values indicate increases (red nuances) in the MCI group. The red arrows and the white outlines denote clusters surviving family-wise error correction for multiple comparisons at $\alpha = .001$. Violin plots, with group mean (black dot) and 95% confidence interval, show the region of interest means extracted from the most significant cluster or in the case of no surviving clusters, the most significant region fulfilling the required minimum cluster extent-threshold. The regions of interest are highlighted in red on the smaller binary maps. Aβ+ was defined by an atlas based Pittsburgh Compound B standard uptake value ratio above 1.5, using mean cerebellar uptake for reference. CBF: cerebral blood flow, CBV: cerebral blood volume, P_tO_2: the tissue oxygen tension required to sustain the minimum metabolic demand of resting brain tissue (2.5 mL/100 mL/min), given the measured MTT and CTH, RTH: relative transit-time heterogeneity (RTH = CTH:MTT)

ers have reported regional reductions in CBF in MCI and in AD,[45,46] and reductions in CBV in AD.[47,48] Previous studies did not find CBV reductions in MCI.[47,48] As these studies did not establish the Aβ status of their MCI subjects, we speculate that the inclusion of non-pAD cases in this more heterogeneous sample may have contributed to this discrepancy.

There are several limitations to our study. We were not able to investigate perfusion in subcortical gray matter due to pulsation and susceptibility imaging artifacts in the DSC-MRI data. Also, to achieve a sufficient temporal and spatial resolution, the coverage of the SE DSC-MRI scans was limited, leaving out inferior parts of the temporal lobe, the cerebellum and superior parts of the frontal and parietal lobes. Therefore, we could not characterize the circulation in these brain regions. Our experimental protocol also did not allow us to relate our findings to any blood brain barrier breakdown present, which has been reported in the hippocampus of subjects with MCI.[49] Of note, females were overrepresented in the healthy control group. Scrutinizing the recruitment procedure offered no clear explanation to this, but we adjusted all statistical models accordingly. Our study also included a relatively small series of subjects, limiting the statistical power of our results. The disease effects we report in this exploratory study therefore need to be validated in larger cohorts, preferably using a longitudinal design to follow the evolution of microvascular flow disturbances relative to amyloid deposition over time.

In conclusion, our study suggests that disturbances in cortical microvascular flow patterns and concurrent hypoperfusion combine to reduce cortical tissue oxygenation in subjects with pAD (Aβ+ MCI), prior to cortical atrophy. We speculate that capillary dysfunction is an early feature of the pathophysiological processes that precedes neurodegeneration and contributes toward driving the conversion of pAD to dementia. Due to the intrinsic vasoconstrictive properties of Aβ,[36,50] future studies should interrogate the cause of capillary dysfunction with a particular focus on its association with cerebral Aβ accumulation and AD risk factors.

ACKNOWLEDGMENTS

We thank radiographers Dora Grauballe and Michael Geneser for help with acquiring MRI, and Irene Klærke Mikkelsen for providing technical support during data processing.

CONFLICTS OF INTEREST

The Authors declare that there is no conflict of interest.

FUNDING

This study was supported by a research grant from The Danish Council for Independent Research, [grant number DFF-4004-00305]. LØ received funding from the VELUX Foundation (ARCADIA—Aarhus Research Center for Aging and Dementia) and from the EU Joint Pro-

gramming initiative within Neurodegenerative Diseases, funded by the Danish Strategic Research Council (APGeM—Pre-clinical genotype-phenotype predictors of Alzheimer's disease and other dementias [grant number 3056-00001]).

REFERENCES

1. Hardy J, Selkoe DJ. The amyloid hypothesis of Alzheimer's disease: progress and problems on the road to therapeutics. *Science*. 2002;297:353-356.
2. Iadecola C. The overlap between neurodegenerative and vascular factors in the pathogenesis of dementia. *Acta Neuropathol*. 2010;120:287-296.
3. Zlokovic BV. Neurovascular pathways to neurodegeneration in Alzheimer's disease and other disorders. *Nat Rev Neurosci*. 2011;12:723-738.
4. Kapasi A, Schneider JA. Vascular contributions to cognitive impairment, clinical Alzheimer's disease, and dementia in older persons. *Biochim Biophys Acta*. 2016;1862:878-886.
5. Hirao K, Ohnishi T, Hirata Y, et al. The prediction of rapid conversion to Alzheimer's disease in mild cognitive impairment using regional cerebral blood flow SPECT. *Neuroimage*. 2005;28:1014-1021.
6. Ruitenberg A, den Heijer T, Bakker SLM, et al. Cerebral hypoperfusion and clinical onset of dementia: the Rotterdam Study. *Annals of neurology*. 2005;57:789-794.
7. Jespersen SN, Ostergaard L. The roles of cerebral blood flow, capillary transit time heterogeneity, and oxygen tension in brain oxygenation and metabolism. *J Cereb Blood Flow Metab*. 2012;32:264-277.
8. Ostergaard L, Sorensen AG, Chesler DA, et al. Combined diffusion-weighted and perfusion-weighted flow heterogeneity magnetic resonance imaging in acute stroke. *Stroke*. 2000;31:1097-2103.
9. Farkas E, Luiten PG. Cerebral microvascular pathology in aging and Alzheimer's disease. *Prog Neurobiol*. 2001;64:575-611.
10. Ostergaard L, Jespersen SN, Mouridsen K, et al. The role of the cerebral capillaries in acute ischemic stroke: the extended penumbra model. *J Cereb Blood Flow Metab*. 2013;33:635-648.
11. Ostergaard L, Aamand R, Gutierrez-Jimenez E, et al. The capillary dysfunction hypothesis of Alzheimer's disease. *Neurobiol Aging*. 2013;34:1018-1031.
12. Ostergaard L, Sorensen AG, Kwong KK, Weisskoff RM, Gyldensted C, Rosen BR. High resolution measurement of cerebral blood flow using intravascular tracer bolus passages. Part II: experimental comparison and preliminary results. *Magn Reson Med*. 1996;36:726-736.
13. Mouridsen K, Hansen MB, Ostergaard L, Jespersen SN. Reliable estimation of capillary transit time distributions using DSC-MRI. *J Cereb Blood Flow Metab*. 2014;34:1511-1521.
14. Angleys H, Ostergaard L, Jespersen SN. The effects of capillary transit time heterogeneity (CTH) on brain oxygenation. *J Cereb Blood Flow Metab*. 2015;35:806-817.
15. Eskildsen SF, Gyldensted L, Nagenthiraja K, et al. Increased cortical capillary transit time heterogeneity in Alzheimer's disease: a DSC-MRI perfusion study. *Neurobiol Aging*. 2017;50:107-118.
16. Nielsen RB, Egefjord L, Angleys H, et al. Capillary dysfunction is associated with symptom severity and neurodegeneration in Alzheimer's disease. *Alzheimers Dement*. 2017;13:1143-1153.
17. Petersen RC. Mild cognitive impairment as a diagnostic entity. *J Intern Med*. 2004;256:183-194.
18. Parbo P, Ismail R, Hansen KV, et al. Brain inflammation accompanies amyloid in the majority of mild cognitive impairment cases due to Alzheimer's disease. *Brain*. 2017;140:2002-2011.
19. Marques JP, Kober T, Krueger G, van derZwaag W, Van de Moortele PF, Gruetter R. MP2RAGE, a self bias-field corrected sequence for improved segmentation and T1-mapping at high field. *Neuroimage*. 2010;49:1271-1281.
20. Vincent RD, Neelin P, Khalili-Mahani N, et al. MINC 2.0: a flexible format for multi-modal images. *Front Neuroinform*. 2016;10:35.
21. Hammers A, Allom R, Koepp MJ, et al. Three-dimensional maximum probability atlas of the human brain, with particular reference to the temporal lobe. *Hum Brain Mapp*. 2003;19:224-247.
22. Aubert-Broche B, Fonov VS, Garcia-Lorenzo D, et al. A new method for structural volume analysis of longitudinal brain MRI data and its application in studying the growth trajectories of anatomical brain structures in childhood. *Neuroimage*. 2013;82:393-402.
23. Coupe P, Manjon JV, Fonov V, Pruessner J, Robles M, Collins DL. Patch-based segmentation using expert priors: application to hippocampus and ventricle segmentation. *Neuroimage*. 2011;54:940-954.
24. Eskildsen SF, Ostergaard LR. Active surface approach for extraction of the human cerebral cortex from MRI. *Med Image Comput Comput Assist Interv*. 2006;9:823-830.
25. Smart SD, Firbank MJ, O'Brien JT. Validation of automated white matter hyperintensity segmentation. *J Aging Res*. 2011;2011:391783.
26. Yushkevich PA, Piven J, Hazlett HC, et al. User-guided 3D active contour segmentation of anatomical structures: significantly improved efficiency and reliability. *Neuroimage*. 2006;31:1116-1128.
27. Mouridsen K, Christensen S, Gyldensted L, Ostergaard L. Automatic selection of arterial input function using cluster analysis. *Magn Reson Med*. 2006;55:524-531.
28. Boxerman JL, Hamberg LM, Rosen BR, Weisskoff RM. MR contrast due to intravascular magnetic susceptibility perturbations. *Magn Reson Med*. 1995;34:555-566.
29. Speck O, Chang L, DeSilva NM, Ernst T. Perfusion MRI of the human brain with dynamic susceptibility contrast: gradient-echo versus spin-echo techniques. *J Magn Reson Imaging*. 2000;12:381-387.
30. Engedal TS, Hjort N, Hougaard KD, et al. Transit time homogenization in ischemic stroke—A novel biomarker of penumbral microvascular failure?. *J Cereb Blood Flow Metab*. 2018;38:2006-2020.
31. Sette G, Baron JC, Mazoyer B, Levasseur M, Pappata S, Crouzel C. Local brain haemodynamics and oxygen metabolism in cerebrovascular disease. Positron emission tomography. *Brain*. 1989;112(Pt 4):931-951.
32. Eskildsen SF, Østergaard LR. In: Jung CR, Walter M, eds. Evaluation of Five Algorithms for Mapping Brain Cortical Surfaces. Campo Grande, Brazil. Washington, DC: IEEE Computer Society Press; 2008:137-144.
33. Worsley KJ, Marrett S, Neelin P, Vandal AC, Friston KJ, Evans AC. A unified statistical approach for determining significant signals in images of cerebral activation. *Hum Brain Mapp*. 1996;4:58-73.
34. Stewart GN. Researches on the Circulation Time in Organs and on the Influences which affect it: parts I.-III. *J Physiol*. 1893;15:1-89.
35. Schumann P, Touzani O, Young AR, Morello R, Baron JC, MacKenzie ET. Evaluation of the ratio of cerebral blood flow to cerebral blood volume as an index of local cerebral perfusion pressure. *Brain*. 1998;121(Pt 7):1369-1379.
36. Nortley R, Korte N, Izquierdo P, et al. Amyloid beta oligomers constrict human capillaries in Alzheimer's disease via signaling to pericytes. *Science*. 2019;365:eaav9518.
37. Kalaria RN. Cerebral vessels in ageing and Alzheimer's disease. *Pharmacol Ther*. 1996;72:193-214.
38. Rasmussen PM, Jespersen SN, Ostergaard L. The effects of transit time heterogeneity on brain oxygenation during rest and functional activation. *J Cereb Blood Flow Metab*. 2015;35:432-442.
39. Thal DR, Griffin WS, deVos RA, Ghebremedhin E. Cerebral amyloid angiopathy and its relationship to Alzheimer's disease. *Acta Neuropathol*. 2008;115:599-609.
40. Park L, Uekawa K, Garcia-Bonilla L, et al. Brain perivascular macrophages initiate the neurovascular dysfunction of alzheimer abeta peptides. *Circ Res*. 2017;121:258-269.
41. Salminen A, Jouhten P, Sarajarvi T, Haapasalo A, Hiltunen M. Hypoxia and GABA shunt activation in the pathogenesis of Alzheimer's disease. *Neurochem Int*. 2016;92:13-24.

42. Oresic M, Hyotylainen T, Herukka SK, et al. Metabolome in progression to Alzheimer's disease. *Transl Psychiatry*. 2011;1:e57.
43. Kisler K, Nelson AR, Rege SV, et al. Pericyte degeneration leads to neurovascular uncoupling and limits oxygen supply to brain. *Nat Neurosci*. 2017;20:406-416.
44. Gutierrez-Jimenez E, Angleys H, Rasmussen PM, et al. Disturbances in the control of capillary flow in an aged APP(swe)/PS1DeltaE9 model of Alzheimer's disease. *Neurobiol Aging*. 2018;62:82-94.
45. Hays CC, Zlatar ZZ, Wierenga CE. The utility of cerebral blood flow as a biomarker of preclinical alzheimer's disease. *Cell Mol Neurobiol*. 2016;36:167-179.
46. Zhang N, Gordon ML, Goldberg TE. Cerebral blood flow measured by arterial spin labeling MRI at resting state in normal aging and Alzheimer's disease. *Neurosci Biobehav Rev*. 2017;72:168-175.
47. Hauser T, Schonknecht P, Thomann PA, et al. Regional cerebral perfusion alterations in patients with mild cognitive impairment and Alzheimer disease using dynamic susceptibility contrast MRI. *Acad Radiol*. 2013;20:705-711.
48. Lacalle-Aurioles M, Mateos-Perez JM, Guzman-De-Villoria JA, et al. Cerebral blood flow is an earlier indicator of perfusion abnormalities than cerebral blood volume in Alzheimer's disease. *J Cereb Blood Flow Metab*. 2014;34:654-659.
49. Montagne A, Barnes SR, Sweeney MD, et al. Blood-brain barrier breakdown in the aging human hippocampus. *Neuron*. 2015;85:296-302.
50. Niwa K, Porter VA, Kazama K, Cornfield D, Carlson GA, Iadecola C. A beta-peptides enhance vasoconstriction in cerebral circulation. *Am J Physiol Heart Circ Physiol*. 2001;281:H2417-H1424.

SUPPORTING INFORMATION

Additional supporting information may be found online in the Supporting Information section at the end of the article.

How to cite this article: Nielsen RB, Parbo P, Ismail R, et al. Impaired perfusion and capillary dysfunction in prodromal Alzheimer's disease. *Alzheimer's Dement*. 2020;12:e12032. https://doi.org/10.1002/dad2.12032